Correlation between saturated fatty acid chain-length and intermolecular forces determined with terahertz spectroscopy

Shuting Fan, Michael T. Ruggiero, Zihui Song, Zhengfang Qian and Vincent P. Wallace

Electronic Supplementary information

THz-TDS experimental methods

Sample preparation

Lauric acid, myristic acid, palmitic acid, stearic acid, and arachidic acid, were purchased from Sigma Aldrich. All samples were used without further purification. The carbon number and melting point of each sample are shown in Table S1. The samples were heated above their melting temperature in a glass beaker and deposited onto a piece of z-cut quartz window. Before recrystallization, another piece of z-cut quartz window parallel to the bottom one was quickly and carefully applied on top of the fatty acid. Three measurements were performed at room temperature on each type of fatty acid by repeating this melting and recrystallization procedure. After the 3rd room temperature measurement of each sample, the temperature of the sample holder was set to 96 K and increased up to 293 K.

Table S1. Sample information

Sample	Carbon number (saturated : unsaturated)	Melting point (°C)[a]
Lauric acid	12:0	44
Myristic acid	14:0	58
Palmitic acid	16:0	63
Stearic acid	18:0	70
Arachidic acid	20:0	77

[a] The melting point may slightly vary depending on the crystal polymorphism.

THz-TDS measurement and data processing

All of the samples recrystallized between the windows within several seconds after the deposition, the thickness of which is unknown. We then adopted a combination of reflection and transmission geometries in the THz measurement. The refractive index was obtained from the reflection measurement without any prior knowledge of the thickness. The detailed calculation method of the reflection setup can be found elsewhere [1, 2]. However, there are challenges to accurately determine the absorption coefficient of low-absorption materials from the reflection geometry [3, 4], especially for solid samples. A transmission measurement was therefore performed on the sample deposited on the window with a piece of bare quartz as the reference (Fig. S1). The thickness of the sample d was determined by minimizing Eq. (1) between 0.2 to 2.5 THz:

$$f(d) = 1 + \left| \frac{c \cdot \Delta\phi}{\omega \cdot d} \right| - n_{rx} \quad (1)$$

where ω is the angular frequency, c denotes the speed of light, $\Delta\phi$ is the phase difference between the sample and reference pulse measured in the transmission geometry, and n_ω is the frequency dependent refractive index obtained from the reflection measurement. The absorption coefficient α is then calculated with the Eq. (2), where $A = \frac{E_{out}^{sample}}{E_{out}^{ref}}$ is the ratio of the amplitude between the sample and reference pulse; t_{23} and t_{32} are the Fresnel coefficients; d is the thickness calculated from Eq. (1).

$$\alpha = -\frac{2}{d}\ln(A \cdot t_{23} \cdot t_{32}) \tag{2}$$

The thickness of each sample in the low temperature measurements using the above method is listed in Table S2.

The absorption coefficient of the three measurements at 293 K calculated with the above mentioned method is shown in Fig. S2.

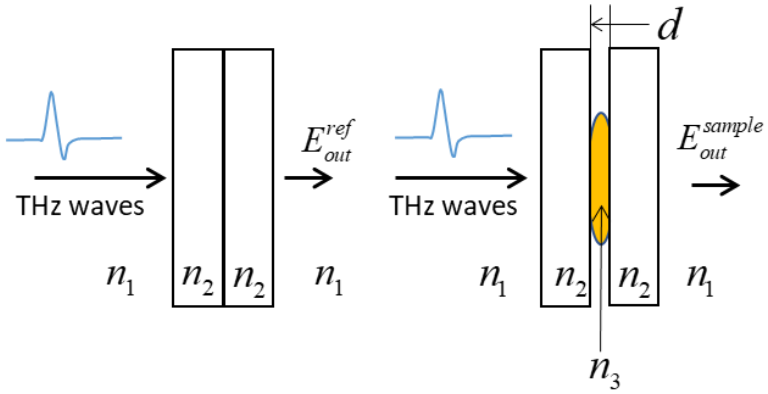

Fig. S1. The reference and sample measurement setup in transmission geometry.

Table 2. Optimized thickness for the deposited samples

Sample	Thickness (μm)
Lauric acid	610
Myristic acid	1165
Palmitic acid	1823
Stearic acid	1359
Arachidic acid	1050

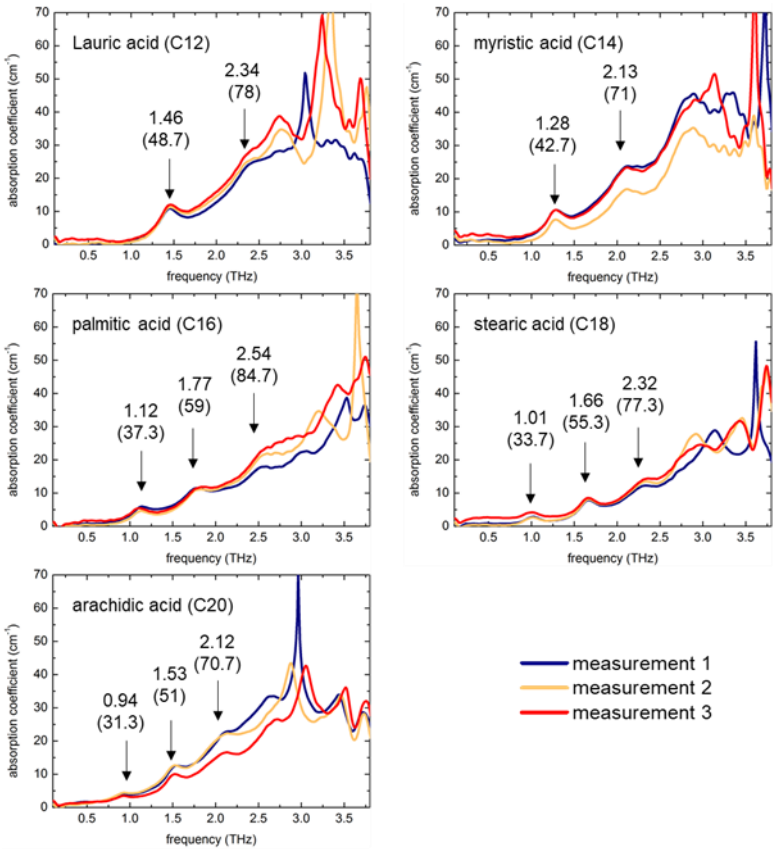

Fig. S2. The absorption coefficient of the fatty acids calculated with the optimization method. The peak location in THz (cm^{-1}) is labelled with arrows.

Powder X-ray Diffraction

Powder X-ray diffraction experiments were performed on the as-received samples using a Rigaku MiniFlex powder x-ray diffractometer using Cu Kα radiation (λ = 1.54056 Å). All of the samples showed characteristic PXRD patterns that indicate no contamination and little-to-no amorphous content. The simulated PXRD patterns based on the experimentally determined single-crystal X-ray diffraction structures are shown for reference as dotted lines. Two samples exhibited preferred orientation effects along the (1 1 1) Miller planes, which have been taken into account when plotting the theoretically-derived patterns.

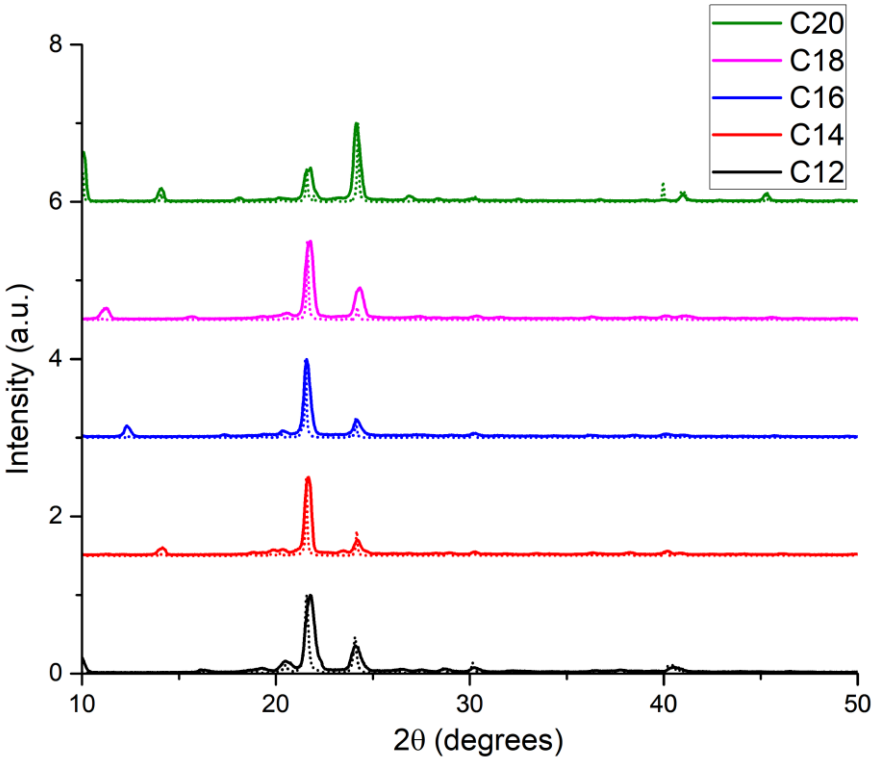

Fig. S3. Experimental (solid) and derived (dotted) PXRD patterns for the saturated fatty acids studied.

Binding Energies and Force Constants

The calculated binding energies were determined by taking the total energy (corrected for basis set superposition error, BSSE) of a single unit cell and subtracting the energy of an extracted single molecule, namely,

$$E_{binding} = \frac{E_{unit\ cell}^{BSSE-Corrected}}{Z} - E_{molecule}$$

The binding energies were scaled by the total number of carbon atoms, which results in a linear relationship between the binding energy and force constants for the lowest-frequency vibrational modes in the frequency bands discussed in text (Fig. S4), as well as between carbon chain length and binding energy (Fig. S5).

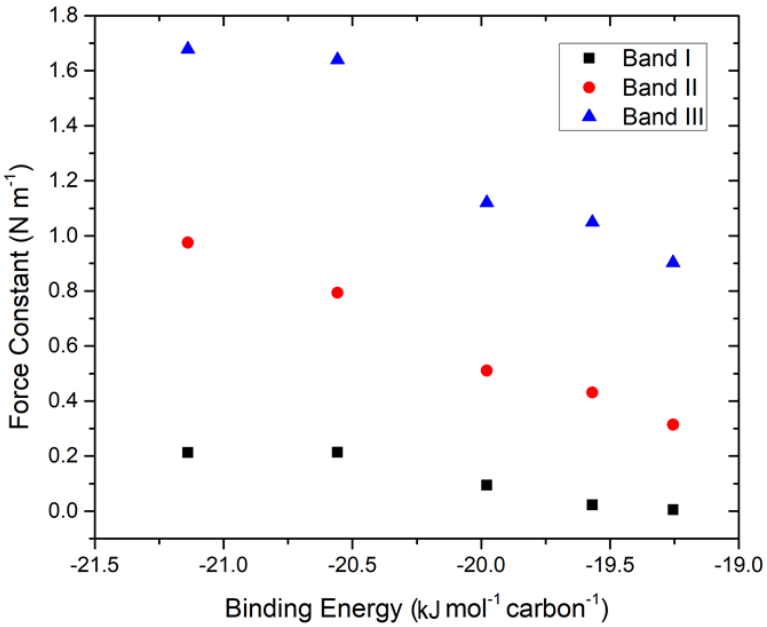

Fig. S4. Relationship between binding energy and the force constants for the lowest frequency modes in the studied fatty acids.

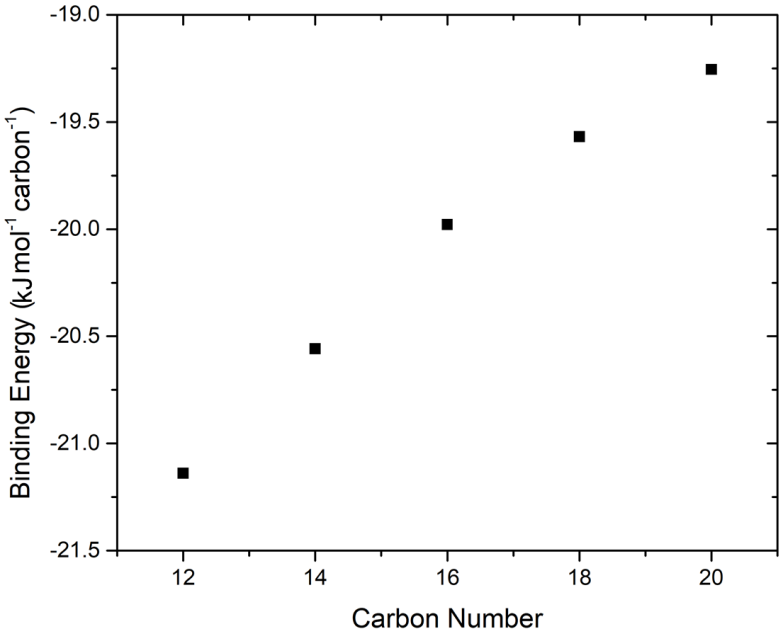

Fig. S5. Relationship between binding energy and length of the carbon chain in the studied fatty acids.

References

1 S. Fan, E. P. J. Parrott, B. S. Y. Ung, E. Pickwell-MacPherson, *Photonics Research,* 2016, *4,* A35.

2 P. U. Jepsen, U. Møller, H. Merbold, *Optics Express,* 2007, ***15,*** 14717-14737.

3 E. M. Vartiainen, Y. Ino, R. Shimano, M. Kuwata-Gonokami, Y. P. Svirko, K. E. Peiponen, *J.Appl.Phys.,* 2004, ***96,*** 4171-4175.

4 A. Pashkin, M. Kempa, H. Němec, F. Kadlec, P. Kužel, *Rev.Sci.Instrum.,* 2003, ***74,*** 4711-4717.